SLOSHING

Odd M. Faltinsen and Olav F. Rognebakke
Department of Marine Hydrodynamics
Norwegian University of Science and Technology
N-7491 Trondheim, Norway

ABSTRACT

Physical aspects of sloshing in ship tanks are discussed. The importance of hydroelasticity for small angles between impacting fluid and body surface is stressed. Performance requirements for numerical methods are presented. CFD methods are reviewed. The drawbacks are long simulation time, sensitivity to numerical parameters and general inability to predict impact loads and resulting structural response. An analytically based sloshing model is therefore recommended. Its drawbacks are that the tank has to be smooth with vertical sides at the free surface. Shallow fluid phenomena are excluded. The method consists of a basic method that assumes infinite tank roof height and a second part, which accounts for tank roof impact. The importance of tank roof impact damping on sloshing is demonstrated. Extensive validation of free surface elevation, total forces and moments for 2-D flow in rectangular and prismatic tanks are reported. This includes realistic motion excitation and studies close to critical depth 0.3374 times the tank breadth.

INTRODUCTION

A partially filled tank will experience violent fluid motion when the ship motions contain energy in the vicinity of the highest natural period for the fluid motion inside the tank. Impact between the fluid and the tank roof is then likely to occur for larger filling ratios. The consequence is wave breaking, spray and mixing of air (or gas) and fluid. Actually, extreme cases with air bubbles everywhere in the fluid have been experimentally observed.

The resonant fluid motion has different main characteristics depending on the fluid depth and the three-dimensionality of the flow. Swirling (rotational) motion is a special feature of 3-D flow ([1],[2]). Our focus is on the highest sloshing period, 2-D flow and finite fluid depth. It implies that typical shallow water phenomena like travelling waves and hydraulic bores are excluded [3].

Since sloshing is a typical resonance phenomenon, it is not necessarily the most extreme ship motions or external wave loads that cause the most severe sloshing. This implies that external wave induced loads can in many practical cases be described by linear theory. However, nonlinearities must be accounted for in the tank fluid motions. Since it is the highest sloshing period (natural period) that is of prime interest, vertical tank excitation is of secondary importance.

Generally speaking the larger the tank size is and the less internal structures obstructing the flow in the tank are present, the more severe sloshing is. The reasons are: a) Increased tank size tends to increase the highest natural sloshing period and hence higher sea states and larger ship motions will excite the severe sloshing. b) Internal structures dampen the fluid motions.

[4] reported damages due to sloshing in bulk carriers, combination Oil-Bulk-Ore (OBO) carriers and LNG carriers. Large and smooth tanks characterized these. Partial fillings in LNG carriers are a consequence of boil-off of gas during operations. Sloshing has always been an important design criterion for oil tankers even if partial filling is rare in actual operation. Since environmental concerns have caused requirements about double hull tankers and ship owners do not want to use internal structures in cargo tanks for easier cleaning, this has lead to wide and smooth oil tanks that increase the probability of severe sloshing. Sloshing is also of concern for Floating Production Storage and Offloading (FPSO) units and shuttle tankers. However, this is for shuttle tankers only in a limited time during loading. Obviously the severity of sloshing is connected to possible filling height restrictions for oil tankers, gas carriers, shuttle tankers and FPSOs. Since ballast exchange is required outside the port for a bulk carrier, there are possibilities for slamming damages. Damage to the hatch cover is of particular concern.

The hydrodynamic loads occurring inside a tank are often classified as impact loads and “dynamic” loads. Impact loads are of course also dynamic loads. But in this context dynamic loads mean loads that have dominant time variations on the time scale of the sloshing period, while impact loads may only last 10^{-2} to 10^{-3} seconds. Both resulting fatigue and ultimate strength are of concern.

Local structural response due to fluid impact (slamming) is an important response variable. But loads on possible internal stringers, web-frames, cross-

ties, piping supports and equipment like LNG pump towers must also be considered. Since some internal structures like a web-frame at the tank roof may be out of the fluid at certain time intervals, impact as well as dynamic loads may matter. Dynamic pressures on the tank wall and bottom as well as total dynamic loads on the tank are also of interest. The latter is needed to estimate tank support reactions and possible global interactions with the ship dynamics. For instance, the horizontal but not the vertical support reaction is important for spherical LNG tanks. Anti-rolling tanks exemplify that global interaction between the tank fluid motion and ship motion, i.e. rolling, can be strong. If several tanks are partially filled like it may be on a FPSO, global ship motions and wave bending moments may be strongly affected.

The following study will concentrate on numerical methods and validation, but starts out stating performance requirements of numerical methods and physical aspects of sloshing.

PHYSICAL AND MATHEMATICAL MODELING

A theoretical method has to be robust and time efficient. Long time simulations are needed to obtain statistical estimates of the tank response. This should ideally be coupled with the ship motions in a stochastic sea. Both impact and non-impact loads should be evaluated. Impact loads may require hydroelastic analysis. There is a variety of tank shapes. This includes rectangular, prismatic, tapered and spherical tanks as well as horizontal cylindrical tanks. The fluid may be oil, liquefied gas, water or heavy density cargoes like molasses and caustic soda. The fluid dynamic properties of the two last cargo types are not focused on in this context. Ideally one should be able to predict two phase flow due to strong mixing of air (or gas) with the fluid. However, this is not focused on. It is hard enough to predict one phase flow.

Internal structures obstructing the flow may be present. This causes flow separation and implies that Navier-Stokes equations have to be solved. The question of turbulence modeling arises, but may not be a dominant effect when flow separation from sharp corners occurs. The argument is that dominant scale effects due to difference between laminar and turbulent flow for separated flow past a blunt body is due to differences in separation line position (or point for 2-D flow). On the other hand the wake behind an internal structural part may interact with another internal structure, the free surface and the tank boundaries. A wake flow would in practice be turbulent. What turbulence model to use is still a research issue. Numerical simulations of flow separation from sharp corners require fine gridding in the vicinity of the corners. The main effect of viscosity for a smooth tank with conventional fluid like oil is normally concentrated in thin boundary layers along the tank boundaries. The boundary layer flow may be laminar in model scale, but is turbulent in full scale. But anyway the boundary layer flow has a negligible influence on tank response of practical interest. It implies that Euler equations can be used for a smooth tank. Further compressibility of the fluid is of secondary importance. Anyway a smooth tank would give the most violent response and provide a conservative estimate if internal structures are present. It is also possible to provide

estimates of the effect of internal structures in combination with potential flow. It assumes the cross-dimensions of the internal structures are small relative to fluid depth and tank breadth. The internal structures are then handled as appendages with Morison type calculations [5]. Equivalent damping of the fluid motion has to be introduced in a similar way as described later in connection with tank roof impact damping.

The previous discussion assumes a submerged internal structure. Some internal structures may be part of the time in and out of the fluid. Fluid impact becomes then part of the problem. The impact pressures can become very high. [2] reported full scale measured pressures up to 24 bar in an OBO tank. We will in the following text discuss fluid impact in a more general sense. Different physical effects occur during slamming. When the local angle between the fluid surface and the body surface is small before impact, an air (or gas) cushion may be formed between the body and the fluid. Compressibility influences the airflow. The airflow interacts with the fluid flow, which is influenced by the compressibility of the fluid. When the air cushion collapses, air bubbles are formed. Air bubbles may also be entrapped in the fluid from previous impacts. The ullage pressure influences the presence and behaviour of air bubbles. The large loads that can occur during impact when the angle between the fluid surface and body surface is small can cause important local dynamic hydroelastic effects. The vibrations can lead to subsequent cavitation and ventilation. These physical effects have different time scales. The important time scale from a structural point of view is when maximum stresses occur. This scale is given by the highest wet natural period (T_{n1}) for the local structure. Compressibility and the formation and collapse of an air cushion are important initially and normally in a time scale smaller than the time scale of when local maximum stresses occur. Hence, the effect on maximum local stress is generally small. The theoretical and experimental studies of wave impact on horizontal elastic plates of steel and aluminium presented by [6], [7], [8], [9] and [10] are relevant in this context. Significant dynamic hydroelastic effects were demonstrated. The physics can be explained as follows. The plate experiences a large force impulse during a small time relative to the highest natural period for the plate vibrations. (Structural inertia phase). This causes the space-averaged relative velocity between the elastic vibration velocity and the rigid body impact velocity V to be zero at the end of the initial phase. The plate then starts to vibrate as a free vibration with an initial vibration velocity V and zero deflection. Maximum strains occur during the free vibration phase. The details of the pressure distribution during the first initial phase are not important. Very large pressures that are sensitive to small changes in the physical conditions, may occur in this phase. This can be seen from the collection of measured maximum pressures during the tests. The measured maximum strains showed a very small scatter for given impact velocity and plate even if maximum pressure varied strongly. The largest measured pressure was approximately 80 bar for V equal to 6 m/s.

Fluid impact against a horizontal tank roof during sloshing has similarities with water impact of elastic plates. The tank roof impact will also cause hydroelastic vibrations in the tank wall adjacent to the impact area. [11] studied this by a hydroelastic beam theory. The effect of a chamfered tank roof was

also investigated. This problem is similar to water entry of a wedge before the horizontal roof part is reached. The effect of hydroelasticity decreases with increasing deadrise angle of the wedge. The tank roof impact causes also damping of the fluid motions. This will be further discussed later in the text.

[12] studied the relative importance of hydroelasticity for an elastic hull with wedge-shaped cross-sections penetrating an initially cal+m water surface. A stiffened plating between two rigid transverse frames was examined. A parameter that is proportional to the ratio between the wetting time of the rigid wedge and the natural period of a longitudinal stiffener, was introduced to quantify the relative importance of hydroelasticity. We can associate the wetting time of the wedge with the duration of the loading. If we make an analogy to a simple mechanical system consisting of a mass and spring, then we know that the duration of the loading relative to the natural period characterizes dynamic effects. The wetting time depends on the impact velocity V and deadrise angle b. It means that the importance of hydroelasticity increases with increasing V and decreasing b. In practice we should be aware of hydroelastic effects when $b <\approx 5°$.

The literature on sloshing contains many studies on slamming pressures. There is a strong tendency to focus on the high slamming pressures that can occur. Few seem to be aware of the importance of hydroelasticity. It is misleading to use physical pressures as parameter for structural response when the pressures become high and concentrated in time and space. What we are saying is that the structure needs time to react. The previous discussion on fluid impact has severe consequences for how sloshing should be numerically modeled.

It has become popular to use CFD to model sloshing. The problem has to be solved in the time domain due to the strong nonlinearities associated with the free surface conditions. There is a broad variety of numerical methods. The load committee of the 13th ISSC has provided a survey in 1997. Normally the Reynolds Averaged Navier Stokes equations (RANSE) are solved, but also Euler equations or potential flows for incompressible fluid are used. 2-D flow studies are most common. The field equations are numerically solved by either Finite Difference Methods (FDM), Finite Volume Methods (FVM) or Finite Element Methods (FEM). The use of Boundary Element Methods (BEM) is based on a velocity potential satisfying Laplace equation. Methods based on field discretization can handle nonlinear free surface motion by height function method, marker method, volume of fluid method or a level set technique.

More recently some meshless methods have been developed to deal with large deformations and even fragmentation of the free surface. Among these, Smoothed Particle Hydrodynamics (SPH) [13] is currently under testing for sloshing problems by Landrini and Colagrossi at INSEAN, Italy. A good agreement with BEM solutions up to breaking has been obtained. Long time simulation for cases with large excitation amplitudes show the ability to follow the post breaking behaviour.

What are then the disadvantages and advantages of using CFD? Advantages are that complex tank geometries, any fluid depth and general excitation may in principle be considered. A CFD method may provide good flow visualization. Flow separation around internal structures can be simulated

by a RANSE-code. A disadvantage is that the CFD methods are time consuming which makes statistical estimates of tank response variables difficult. Some methods may not be robust enough. For instance a Boundary Element Method based on mixed Eulerian-Lagrangian method breaks down when an overturning wave hits the free surface. Numerical problems may also arise with a BEM at the intersection between the free surface and the tank boundary. [14] discussed numerical problems associated with BEM and sloshing. If not sufficient care is shown, some of the methods may numerically loose or generate fluid mass on a long time scale. Since the highest natural period of the fluid motion is strongly dependent on fluid mass, this can result in an unphysical numerical simulation. This was demonstrated by Solaas [15] by using the commercial, multipurpose FLOW-3D code, developed by Flow Science, Inc. The method uses a combination of the SOLA finite difference scheme for solving Navier-Stokes equations and the Volume of Fluid (VOF) technique for tracing the free boundaries of the fluid. Kim [16] has presented a CFD method where conservation of fluid mass is satisfied. The amount of fluid in the tank is corrected for each time step by slightly moving the free surface. The correction is so small that the global motion is not affected.

It seems generally accepted that CFD codes have difficulties in predicting impact loads. This was also the conclusion of the load committee of 13th ISSC in 1997. A reason is rapid changes in time and space occurring even for relatively large local angles between the impacting free surface and the body surface ([17]). Few codes include hydroelasticity during impact. However, if doing so, the structural modeling requires also special care. [9] demonstrated the numerical difficulties in modeling hydroelastic impact of a horizontal beam. The complications are associated with the many structural modes that are initially excited and the very rapid change of the wetted body surface. More analytically based methods were therefore used to provide robust solutions.

There exist examples on satisfactory predictions of non-impact loading by CFD (f. ex. [15] and [18]). However the load committee of the 13th ISSC presented a comparative study by 12 different CFD codes belonging to different classification societies, a shipyard, research organizations and universities. The agreement in predicted free surface elevations in non-extreme cases was not convincing.

[15] illustrated the grid dependence and the sensitivity to parameters used in numerical differentiation and iteration procedures in the FLOW-3D code. The EPSADJ parameter gives an automatic adjustment of the convergence criterion in the pressure iteration algorithm in order to fulfill the continuity equation. The default value is 1.0, but a much smaller value had to be used for resonant fluid motion to satisfy mass conservation. But even so the results were not perfect. A case with EPSADJ=0.01 showed that the volume error was 4% after 30 oscillation periods. This illustrates also the problem of using a multipurpose program. The different main applications have different main important physical effects. The ALPHA parameter in FLOW-3D controls the weighting of the advective flux terms in Navier-Stokes equation. ALPHA can be between 0 and 1. The default value is 1.0, which means fully upstream differencing and a first order approximation of the advective flux terms is used. ALPHA=0.0 means central differencing, but this gave a numerically unstable solution. It is difficult

from a physical point of view to state that the default value ALPHA=1.0 should be used for sloshing. [15] demonstrated that there could be a large sensitivity to choice of parameters and grid size. Convergence studies by decreasing the grid size were performed. This gives a qualitative but not quantitative guidance on how to select grid size. The reasons are that convergence is dependent on the ALPHA parameter and that in some cases the results did not converge by decreasing grid size. There is of course also a limit to how small the grid size can be before the demand on computer resources gets too large.

Instead of developing a CFD code we have decided to develop a more analytically based method. The method is time efficient and seems easy to combine with the ship motions and external linear wave induced loads. The simulation time depends on the chosen approximate modal model and excitation parameters. Consider for instance a typical calculation of 100 forced motion oscillation periods presented later in the paper. This may take from 1 to 20 seconds on a Pentium-III 500. The numbers are based on non-optimized computer code. The fluid depth has to be finite. Our selected procedure applies to any tank shape as long as the tank walls are vertical near the mean free surface. Details have so far been developed for a rectangular 2-D tank and a vertical circular tank. Since irrotational fluid motion is assumed, internal structures causing flow separation can only be treated empirically by Morison type calculations. The basic method assumes infinite tank roof height. The effect of the tank roof impact is handled by generalizing Wagner's method [19]. Since analytically based methods are used, fluid impact load predictions are robust. The effect of hydroelasticity can be incorporated. The method will be described in more details in the next chapter.

ANALYTICALLY BASED SLOSHING MODEL

We describe first the basic method, which assumes infinite tank roof height. Details will be shown for 2-D flow and a rectangular rigid tank. The tank can have a general forced motion in surge (or sway), heave and pitch (or roll), but the main frequency component s of the forced oscillation has to be in the vicinity of the lowest natural frequency s_1 for the tank fluid motion. The fluid is incompressible and the flow is irrotational. The fluid depth and the breadth of the tank are h and l. The coordinate system (x, z) is fixed relative to the tank with origin in the mean free surface and the center of the tank (See Fig. 1). The procedure is based on a Bateman-Luke variational principle and use of the pressure in the Lagrangian of the Hamilton principle. This results in a system of nonlinear ordinary differential equations in time. The unknowns are generalized coordinates b_i of the free surface elevation. The free surface elevation z is written as

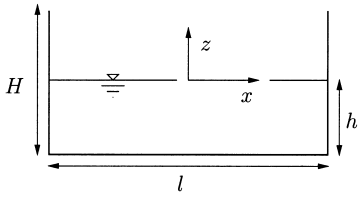

Figure 1: Coordinate system and tank dimensions

$$z = \sum_{i=1}^{N} b_i(t)\cos\left(\frac{pi(x+0.5l)}{l}\right) \tag{1}$$

Since Eq. 1 assumes z to be a single valued function of x, it implies no overturning waves and vertical tank sides in the free surface. Further Eq. 1 does not permit travelling waves. The consequence is that shallow water conditions cannot be simulated. The forced oscillation amplitude is assumed small and of $O(e)$. There exist different possibilities for how to order b_i, but it should reflect that the fluid response is lower order than $O(e)$. This reflects that a strong amplification of the flow occurs due to a small excitation. However, in order to develop an asymptotic theory, we must assume z to be asymptotically small. The original method presented by Faltinsen et al. [20] assumed $b_i = O(e^{i/3})$, $i = 1,3$. Higher order terms than e are neglected in the nonlinear equations. The following system of nonlinear ordinary differential equations for the generalized coordinates describing the free surface are derived for forced motions

$$\begin{aligned}
&\left(\ddot{b}_1 + s_1^2 b_1\right) + d_1\left(\ddot{b}_1 b_2 + \dot{b}_1 \dot{b}_2\right) + d_2\left(\ddot{b}_1 b_1^2 + \dot{b}_1^2 b_1\right) \\
&\qquad + d_3 \ddot{b}_2 b_1 + P_1(\dot{v}_{0x} - S_1 \dot{w} - gy\ ) + Q_1 \dot{v}_{0z} b_1 = 0 \\
&\left(\ddot{b}_2 + s_2^2 b_2\right) + d_4 \ddot{b}_1 b_1 + d_5 \dot{b}_1^2 + Q_2 \dot{v}_{0z} b_2 = 0 \\
&\left(\ddot{b}_3 + s_3^2 b_3\right) + d_6 \ddot{b}_1 b_2 + d_7 \ddot{b}_1 b_1^2 + d_8 \ddot{b}_2 b_1 + d_9 \dot{b}_1 \dot{b}_2 \\
&\qquad + d_{10} \dot{b}_1^2 b_1 + P_3(\dot{v}_{0x} - S_3 \dot{w} - gy\ ) + Q_3 \dot{v}_{0z} b_3 = 0 \\
&\ddot{b}_i + s_i^2 b_{ii} + P_i(\dot{v}_{0x} - S_i \dot{w} - gy\ ) + Q_i \dot{v}_{0z} b_i = 0, \quad i \geq 4
\end{aligned} \tag{2}$$

Here dots mean time derivatives. v_{0x} and v_{0z} are projections of translational velocity onto axes of Oxz, $w(t)$ and $y(t)$ are the angular velocity and angle of coordinate system $Oxyz$ with respect to an earth fixed coordinate system. Both v_{0x} and w cannot be zero. g means acceleration of gravity. The calculation formulas for the coefficients s_i, P_i, S_i, Q_i, $i \geq 1$ and d_j, $j = 1,\ldots,10$ are given in Faltinsen et al. [20]. s_i means the natural frequencies. The equation system is solved numerically by a fourth order Runge-Kutta method.

Faltinsen & Timokha [21] found that the excitation amplitude had to be very small and that the depth should not be close to the critical value $h/l = 0.3374$ in order for Eqs. 2 to be valid. This was explained to be due to secondary resonance. An example of such mechanisms is as follows. Nonlinearities cause oscillations with frequency $2s$, where s is the excitation frequency of the rigid body motion. If the second natural frequency s_2 of the fluid is close to $2s$, secondary resonance will occur. The generalized coordinate b_2 will be amplified and can be of same order as b_1. Nonlinear interactions can also cause resonant oscillations at the other natural frequencies. If the excitation amplitude is increased, the fluid response becomes large in an increased frequency domain around the first natural frequency. This increases the possibility that large nonlinearly excited resonance oscillations at a higher

natural frequency can occur. Both the second and third mode associated with respectively b_2 and b_3 can be the same order as b_1. Since the amplification of the fluid motion is relatively larger at the critical depth than at other fluid depths, the upper bound of tank excitation amplitude where the theory of Faltinsen et al. [20] is applicable for critical depth is relatively small. An adaptive procedure that allows for different ordering of b_i is presented by Faltinsen & Timokha [21]. This worked for all excitation periods as long as $h/l > 0.24$. When $h/l < 0.24$, good agreement with experiments was documented in isolated cases for h/l down to 0.173.

When the water impacts on the tank roof, fluid damping is believed to occur. The hypothesis is that the kinetic and potential energy in the jet flow caused by the impact is dissipated when the jet flow later on impinges on the free surface. The latter process resembles rainfall on water. We will illustrate the procedure by the tank with chamfered tank roof shown in Fig. 3. The upper corner is one half part of a wedge. When the water reaches this corner, the problem is similar to water entry of a wedge. Rognebakke & Faltinsen [22] estimated the damping of sloshing due to tank roof impact, by first evaluating the potential and kinetic energy flux $\mathrm{d}E_{\mathrm{pot}}/\mathrm{d}t$ and $\mathrm{d}E_{\mathrm{kin}}/\mathrm{d}t$ into the jet caused by the impact. The ambient flow was based on [20], but [21] can also be used. This theory gives a time varying impact velocity and radius of curvature R of impacting surface. R has to be large, i.e. run-up cannot be considered. The Wagner theory is convenient to use because a time varying velocity, R and the change from the wedge part to the horizontal part of the roof can be analytically accounted for. The effect of the tank bottom and the opposite wall is negligible (Faltinsen & Rognebakke [23]). Since the Wagner theory overpredicts $\mathrm{d}E_{\mathrm{pot}}/\mathrm{d}t$ and $\mathrm{d}E_{\mathrm{kin}}/\mathrm{d}t$, a correction factor based on the similarity solution by Dobrovol'skaya [24] was introduced. An alternative is to use the generalized Wagner theory presented by Faltinsen [25]. The linear damping terms $2\zeta s_i \dot{b}_i$ are included in each of eqs. 2. The damping is found as an equivalent damping so that the energy ΔE removed from the system during one full cycle is equal to the kinetic and potential energy lost in the impact, i.e. $\zeta = \Delta E/(4\pi E)$. E is the total energy in the system, which is found from $\dot{E} = F_x v_{0x}$ for forced surge motion. Here F_x is the horizontal hydrodynamic force. An iterative procedure is followed. A simulation over one period is started with no damping. A first estimate of ζ is found. The simulation is repeated, which results in a new ΔE and thereafter a new ζ. This is done for iteration $i > 1$ as $0.5(\Delta E_i + \Delta E_{i-1})/E = 4\pi\zeta$. Typically, 5 iterations are sufficient for convergence. The procedure conserves fluid mass, which is essential in sloshing problems. Further, when the basic method and the tank roof impact model are combined, overturning waves are accounted for through the impact model.

Faltinsen et al. [20] presented an extensive validation by comparing with experimental values of free surface elevation in a rectangular tank with 2-D flow. The tank was forced to oscillate in the horizontal direction in the cross-sectional plane with excitation frequency in the vicinity of the lowest natural frequency. It was demonstrated that it takes a very long time for transient fluid

motion to die out when the fluid does not hit the tank roof in a smooth tank. This implies that damping is very low and that viscosity does not matter. Modulated (beating) waves occurred as a consequence of transient and forced oscillations. Strong nonlinearities were evident.

Faltinsen & Timokha [21] presented also an extensive validation for rectangular and prismatic tanks. Steady state values of horizontal force and roll moment amplitudes as well as free surface elevation were studied. The maximum forced surge harmonic oscillation amplitude $|h_1|$ was 0.1 times the breadth and the maximum forced harmonic pitch oscillation amplitude was 0.1 rad. We will present one example and at the same time compare with FLOW-3D calculated by [15] (Fig. 2).

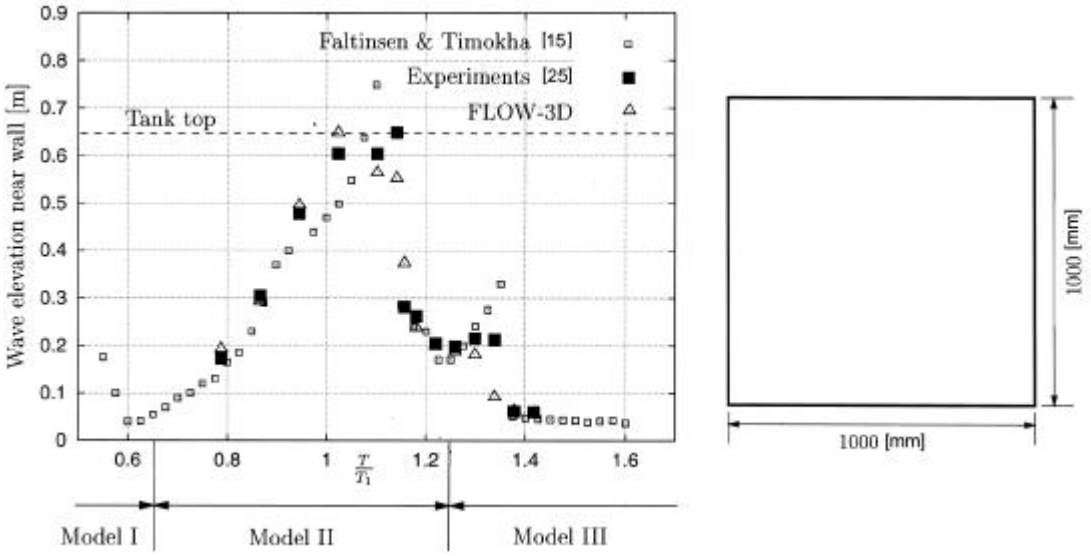

Figure 2: Steady-state maximum wave elevation near the wall vs "forced period (T)-first natural period (T_1) ratio". Rectangular tank with $h/l = 0.35$, $|h_1| = 0.05l$

The fluid depth is 0.35 times the breadth, which is close to the critical depth. The grid size used in the FLOW-3D calculations was $\Delta x = \Delta z = 0.025$ m, where Δx and Δz are respectively the horizontal and vertical distance between adjacent grid points. This means a total of 40×40 elements. The ALPHA and EPSADJ parameters were respectively 0.5 and 1.0. Three different models were used in the adaptive multimodal approach by Faltinsen & Timokha [21]. These correspond to different ordering of the generalized free-surface coordinates b_i (See Eq. 1). The first stage of the analysis by [21] is to locate possible resonances for T/T_1 between 0.45 and 1.65. The primary resonances of the first and third mode occur at respectively $T/T_1 = 1$ and $T/T_1 = 0.55$. The secondary resonance of the second mode is predicted at $T/T_1 = 1.28$. The secondary resonance of the third mode is at $T/T_1 = 1.55$. The positions of primary and secondary resonances are important for selection of model. The models are indicated as Model I,II and III. It was controlled that the models overlap with each other in a small frequency domain. Model I was used for

$0.5 \le T/T_1 \le 0.65$. The expected resonances are due to primary excitation of the third and first mode. They have the same main frequency response s. No secondary resonance is expected. This causes the relations $b_1 \approx b_3 = O(e^{1/3})$. This means that the secondary modes have the main harmonic $2s$. Such modes are $b_2 \approx b_6 = O(e^{2/3})$. Other modes (up to 9th) are considered as driven and having $O(e)$. Model II was used for $0.6 \le T/T_1 \le 1.25$. The system is of third order in b_1 and b_2. It contains all the necessary terms in Eq. 2 as well as a theory considering $b_1 \approx b_2 = O(e^{1/2})$. The modes b_3, b_4, b_5 and b_6 were included as driven. If the response is not too large, the modal system gives the same results as Eqs. 2. When $T/T_1 > 1.28$, the third mode response was assumed to have the same order as b_1 and b_2 (Model III). The reason is the influence of the secondary resonance of third mode at $T/T_1 = 1.55$. Model III was used for $1.28 \le T/T_1 \le 1.65$. The predicted values in Fig. 2 belong to different branches of the steady-state periodic solution. The concept of branches of the solutions was for instance extensively discussed by Faltinsen et al. [20]. There exist in their solution an upper and lower branch. The lower branch is divided into an upper and lower branch. The lower branch is divided into a stable and unstable sub-branch with a turning point between them. A jump in the solution will happen at an excitation period corresponding to the turning point. The results in Fig. 2 have two jumps, one around $T/T_1 = 1.1$ and the other one around $T/T_1 = 1.3$. Fig. 2 shows that the multimodal approach by Faltinsen & Timokha [21] agrees well with the experiments. No tank roof damping was included. Even if the steady-state free surface elevation did not hit the tank roof, impact would occur during the transient phase. The FLOW-3D calculations agree also well with the experiments. However, it should be noted that the results would depend on grid size and the ALPHA and EPSADJ parameters previously discussed.

Horizontal forced harmonic oscillations of the LNG tank in Fig. 3 will now be studied. Two-dimensional fluid motions occur. The mean fluid depth h is $0.4l$ where l is the tank breadth. The forced oscillation amplitude $|h_1|$ is $0.01l$. Fig. 3 shows numerical and experimental predictions of steady-state maximum horizontal force F as a function of the forced oscillation frequency s. The lowest natural frequency s_1 is 4.36 rad/s. Different fluids with different viscosity are used in the experiments. This has small influence on the non-dimensional force. There are two theoretical curves based on Faltinsen & Timokha [21]. One assumes infinite tank roof height and the other one accounts for tank roof damping. The impact-induced horizontal force is not included in the latter case. The effect of the two lower corners submerged in the fluid was neglected. The error in doing so is small ([21]). The previous described Model II and III were used for respectively $0.65 \le T/T_1 \le 1.3$ and $1.3 \le T/T_1 \le 1.65$. Results by FLOW-3D published by [15] are also presented in Fig. 3. The grid size was $\Delta x = 0.0276$ m and $\Delta z = 0.02782$ m corresponding to 50×37 elements. The effect of the corners was accounted for. There are also shown two curves corresponding to ALPHA=1.0 and 0.5. In both cases EPSADJ=0.01 which is

different from the value used in connection with Fig. 2. The presented results for ALPHA=1.0 and 0.5 are clearly different. The results obtained with the default value ALPHA=1.0 are furthest away from the experiments. The agreement between FLOW-3D and the experiments is fair.

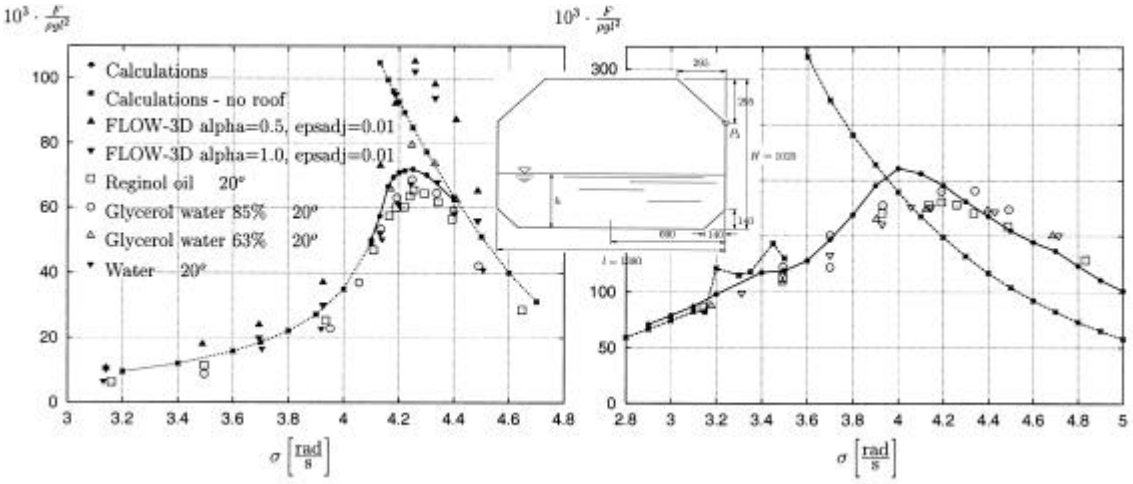

Figure 3: Maximum horizontal force F per unit length of LNG tank as a function of forced oscillation frequency s . Forced surge amplitude $|h_1| = 0.01l$ (left) and $|h_1| = 0.1l$ (right). Mean fluid depth $h = 0.4l$. l =tank breadth, r =mass density of the fluid. Experiments by Abramson et al. [2]. Length dimensions in [mm]

The results based on Faltinsen & Timokha [21] and accounting for tank roof impact are in good agreement with experiments. The simulations with infinite tank roof height give jumps between different solution branches at certain frequencies. These jumps disappear when tank roof impact damping is introduced.

Fig. 3 shows also comparisons between theory and experiments for the larger surge excitation amplitude $|h_1| = 0.1l$. This represents a realistic design excitation. Only the analytically based sloshing models are used. We note the significant effect of tank roof damping when $s > \approx 3.5$ rad/s. Accounting for tank roof impact was not straightforward for $|h_1| = 0.1l$. Very violent motions occurred initially. An artificial damping coefficient was therefore introduced in the transient phase. When steady state oscillations were achieved, our tank roof damping model was switched on. Fig. 3 demonstrates good agreement between theory and experiments. One may note that the sloshing force for $s > \approx 4.0$ rad/s is larger when tank roof impact is included in the calculations. This will be explained by examining the force expression. The horizontal hydrodynamic force for forced surge oscillations can according to [20] and [21] be written as

$$F_x = -m_l \left(\frac{\mathrm{d}v_{0x}}{\mathrm{d}t} + \frac{\mathrm{d}^2 x_C}{\mathrm{d}t^2} \right) \qquad (3)$$

where m_l is the fluid mass and x_C is the instantaneous horizontal position of the mass-centre of the fluid relative to the tank fixed coordinate system. x_C is a function of the generalized coordinates b_i. Fig. 4 shows how the magnitude is increased and the phasing shifts for the term depending on x_C, when impact damping is accounted for. This leads to a larger total hydrodynamic force even if the free surface elevation is smaller.

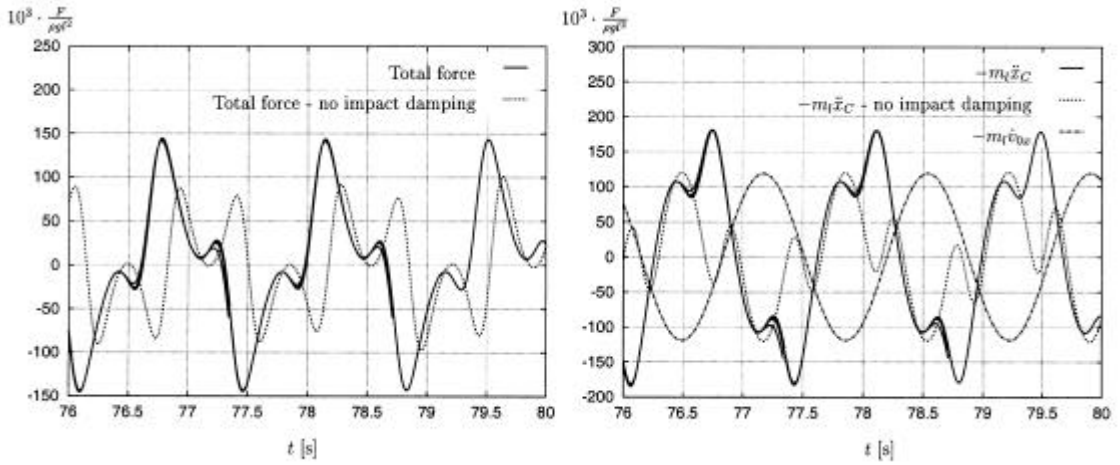

Figure 4: Contributions to the total hydrodynamic force on the LNG tank shown in Fig. 3 for a forced sway frequency $s = 4.6$ rad/s. $|h_1| = 0.1l$

The analytically based method provides a robust procedure for impact loads. However, this has to be validated for cases where impact pressures are relevant for local structural response. Abramson et al. [2] presented experimental slamming predictions for the LNG tank shown in Fig. 3. This included statistical distributions. The pressure transducer location is indicated as P_2 in Fig. 3. Viscosity seemed to be important when the forced surge amplitude $|h_1|$ was 0.01 times the tank breadth l, but not for $|h_1| = 0.1l$. Fig. 5 shows computed and experimental pressures for $|h_1| = 0.1l$. The computations are for steady state motions. The experimental values are 10% exceedance limits for the pressure. The computed values would represent the most frequently occurring in a long time simulation. What the 10% exceedance level would be depends on the time series. We can very well realize the level of pressure shown in Fig. 5 in the transient phase of our computations. But we would need the complete time series in the experiments to make a quantitative estimate of the 10% exceedance limit. The way that the data by Abramson et al. [2] were presented, suggest that they meant that the process is stochastic. However, in our opinion this particular type of impact on a chamfered tank roof is deterministic during harmonic excitation of the tank. Another matter is impact on a horizontal tank roof. In that case the impact pressure may very well have a stochastic behaviour, but as previously discussed, maximum pressure is then an irrelevant parameter for local structural response.

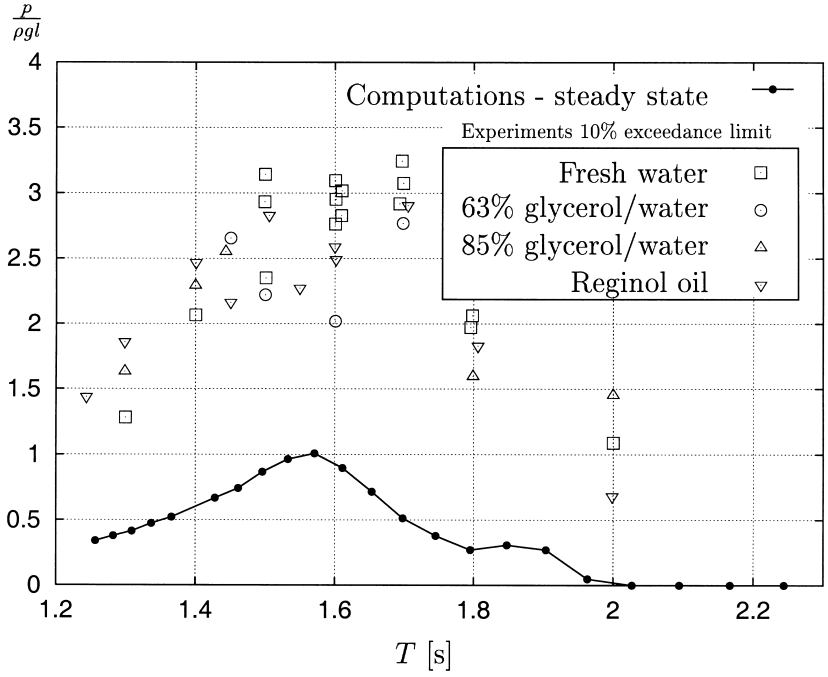

Figure 5: Measured [2] and calculated impact pressures p at the location P_2 in the LNG tank shown in Fig. 3 presented as a function of forced oscillation period T. $|h_1| = 0.1l$

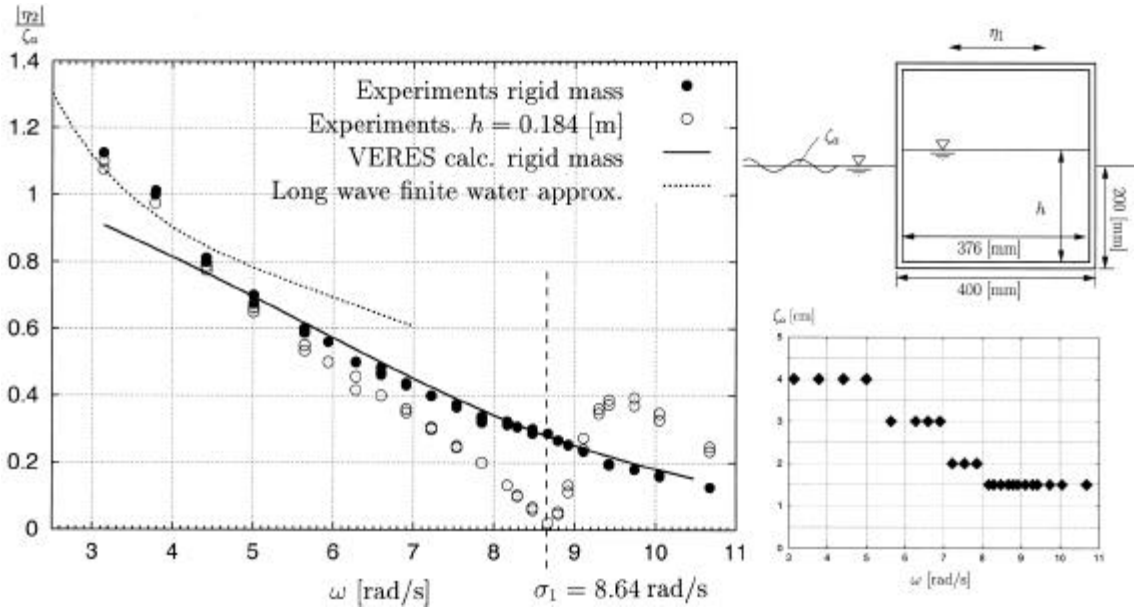

Figure 6: Sway motions of a rectangular ship section in regular beam sea. s_1 is the first natural frequency of the fluid motion in the tanks for $h = 0.184$ m

The analytically based sloshing model facilitates coupling between fluid motion in the tank and wave induced ship motion. Experimental 2-D studies with a ship cross-section containing two tanks have therefore been carried out at the

wave flume of the Department of Marine Hydrodynamics at the Norwegian University of Science and Technology. The wave flume has an overall length of 13.5m and is 0.6m wide. It is equipped with an electronically operated, computer controlled, single flap wavemaker, calibrated for a water depth of 1.03m. The wavemaker has the ability to dampen out waves reflected by the model at the same time as new waves are generated. The rectangular ship section shown in Fig. 6 is free to move in sway. The draught is 0.20m, and the section is excited by regular beam waves with frequency w . The length of the ship model is 0.596m. The mass of the model is adjusted to be equal to the buoyancy for both empty and half-filled tanks. The amplitude z_a of the incoming wave is lowered as the wave frequency increases to have acceptable wave steepness. The relationship between z_a and w is shown in Fig. 6. The model contains two identical tanks with an inner length l=0.376mm. The width of a tank is 0.15m, and the height is 0.388m. The section is prevented from drifting off by two springs with a total stiffness of 30.9 N/m.

Fig. 6 shows calculated and measured values for the sway amplitude $|h_2|$ of the section. The calculations have presently not been performed with fluid inside the tanks. The sway amplitude is normalized by the amplitude of the incoming wave.

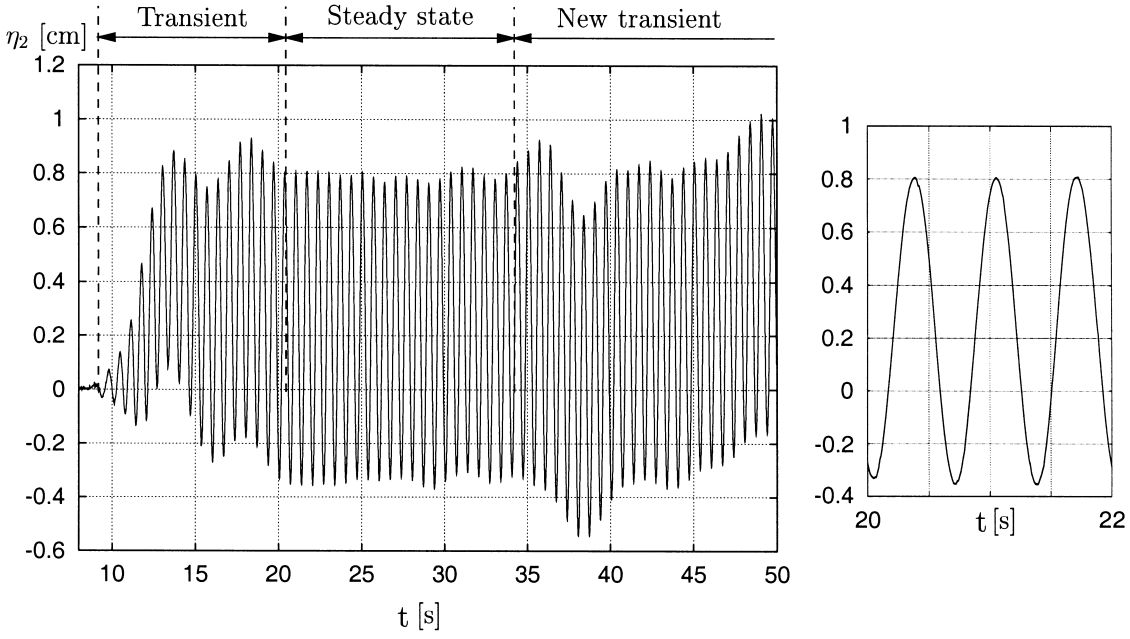

Figure 7: Example of time history of the sway motion of the ship section with fluid in the tank. $w = 9.42$ rad/s and $z_a = 0.015$ m

Fig. 7 shows a typical time history of the measured sway motion of the ship section. First there is a transient phase before the system reach a steady state. A beating period of approx. 5 seconds is evident during the transient phase. This is the eigenperiod for horizontal motion of the system consisting of the springs and the ship model without fluid in the tanks. Due to 2. order drift force a

shift in mean position of the section occurs. The steady state is ended when waves are reflected from the wavemaker and beach at the end of the wave flume and a second transient phase starts. The steady state motions show almost no trace of higher order harmonics. This indicates that the higher order part of the sloshing force is filtered out by the system. The experimental results for rigid mass agree well with the computed values from the linear seakeeping code VERES. In these computations, infinite water depth is assumed. This explains the discrepancy for low frequencies. Calculated results from long wavelength, finite water depth theory show better agreement when the wavelength is long compared to the water depth and section length.

We observe a large effect of the fluid motions inside the tanks for $w >\approx 7$ rad/s. An excitation $w <\approx 9$ rad/s results in a lower sway response for half-filled tanks than for a rigid mass. The resulting force from the fluid motion in the tanks acts then against the sway excitation force. When $w \approx s_n$ there is almost no sway motion. For $w >\approx 9$ rad/s the sway motion is increased due to the filling of the tanks. This behaviour can be explained by using a linear model for the sloshing. We then find that the phase of the horizontal sloshing force shifts 180° when the excitation frequency is changed from being slightly below to slightly above the first natural frequency. This is well known from linear dynamic systems.

CONCLUSIONS AND PERSPECTIVES

Sloshing represents violent fluid motion with strong nonlinearities during resonant motion in the vicinity of the highest natural period. The physical behaviour during impact is discussed. The importance of hydroelasticity for small angles between impacting fluid and body surface is stressed. The very high slamming pressures are then unimportant for the structural response. CFD methods are reviewed. The drawbacks are long simulation time, sensitivity to numerical parameters and general inability to predict strong impact. An analytically based sloshing model is therefore recommended. Its drawbacks are that the tank has to be smooth with vertical sides at the free surface. Shallow fluid phenomena are excluded. However, this can be studied by the method of [3]. This was done with satisfactory results for horizontal forces by Abramson et al. [2] for a 2-D rectangular tank with fluid depth 0.12 times the breadth. The importance of tank roof impact damping on sloshing is demonstrated. Extensive validation of free surface elevation, total forces and moments for 2-D flow in rectangular and prismatic tanks are reported. This includes realistic motion excitation and studies close to critical depth 0.3374 times the tank breadth.

The analytical method provides a robust way to predict impact pressures. However, this has to be validated for cases where impact pressures are relevant for local structural response. The study shows that steady-state impact pressures are clearly lower than would occur during a transient phase.

The structure of our method facilitates coupling with the ship dynamics. Experimental 2-D studies with a ship cross-section containing two tanks are presently performed. These show that the ship response is strongly influenced by the fluid motion in the tanks. The next step is to perform a complete time

domain solution of a ship by combining external linear wave loads with the nonlinear analytically based sloshing model for head and beam sea conditions.

The details of the analytically based method have to be developed for a ship tank with 3-D flow. A 3-D rectangular tank would represent a direct generalization of the 2-D method for a rectangular tank. Analysis can be used to the same extent. However, a tapered tank would require numerical methods to describe the linear eigenfunctions as a part of the solution procedure.

AKNOWLEDGEMENTS

The contributions from Dr. Hang Sub Urm from DNV concerning important sloshing problems are appreciated.

BIBLIOGRAPHY

[1] Abramson, M.N., Chu, W.H., Kana, D.D. : ”Some Studies of Nonlinear Lateral Sloshing in Rigid Containers”, *Journal of Applied Mechanics*, Vol. 33, No. 4, (1966).

[2] Abramson, M.N., Bass, R.G., Faltinsen, O.M., Olsen, H.A. : ”Liquid Slosh in LNG Carriers”, *10th Symp. on Naval Hydrodynamics, Boston*, (1974).

[3] Verhagen, J.H.G, and van Wijngaarden, L. : “Nonlinear Oscillations of Fluid in a Container” , *J. Fluid Mech.,* Vol. 22, Part. 4, (1965).

[4] Hansen, H.R. : ”Damage Experience, Potential Damages, Current Problems Involving Slosh Considerations”, *Seminar on Liquid Sloshing, Det Norske Veritas, Høvik, Norway,* (1976).

[5] Faltinsen, O.M. : ”Sea Loads on Ships and Offshore Structures”, *Cambridge University Press*, (1990).

[6] Faltinsen, O.M. : ”The Effect of Hydroelasticity on Slamming”, *Phil. Trans. R. Soc. Lond.*, A. 355, pp. 575-591, (1997).

[7] Faltinsen, O.M., Kvålsvold, J., and Aarsnes, J.V. : ”Wave Impact on a Horizontal Elastic Plate”, *J. Marine Science and Techn*., Vol. 2, No. 2, pp. 87-100, (1997).

[8] Haugen, E.M. : ”Hydroelastic Analysis of Slamming on Stiffened Plates with Application to Catamaran Wetdeck*”, Dr. Ing. thesis, Dept. Marine Hydrodyn., NTNU, Trondheim, Norway*, (1999).

[9] Kvålsvold, J. : “Hydroelastic Modelling of Wetdeck Slamming on Multihull Vessels”, *Dr. Ing. thesis, Dept. Marine Hydrodynamics, NTH, Trondheim, Norway*, MTA-Report 1994:100, (1994).

[10] Kvålsvold, J., Faltinsen, O.M., Aarsnes, J.V. : “Effect of Structural Elasticity on Slamming Against Wetdecks of Multihull Vessels”, *Proc. PRADS'95, Korea, The Society of Naval Architects of Korea*, pp. 1.684-1699, (1995).

[11] Faltinsen, O.M. : “Slamming on Ships”, Keynote lecture, *IMAM 2000, Naples, Italy*, (2000).

[12] Faltinsen, O.M. : “Water Entry of a Wedge by Hydroelastic Orthotropic Plate Theory” , *J. Ship Research*, Vol. 43, No. 3., pp. 180-193, (1999).

[13] Monaghan, J.J. : “Smoothed Particle Hydrodynamics”, *Annu. Rev. Astron. Astrophys*, Vol. 30, pp. 543-74, (1992)

[14] Landrini, M., Grytøyr, G., Faltinsen, O.M. : "A B-Spline based BEM for Unsteady Free-Surface Flows", *J. Ship Research*, Vol. 13, No. 1, pp. 13-24, (1999).
[15] Solaas, F. : "Analytical and Numerical Studies of Sloshing", *Dr. Ing. thesis, Dept. Marine Hydrodynamics, NTNU, Trondheim, Norway*, (1995).
[16] Kim, Y. : "Numerical Simulation of Sloshing Flows with Impact Load", To be submitted
[17] Zhao, R., and Faltinsen, O.M. : "Water Entry of Two-Dimensional Bodies" , *J. Fluid Mech*., Vol. 246, pp. 593-612, (1993).
[18] Mikelis, N.E., Miller, J.K., Taylor, K.V. : "Sloshing in Partially Filled Liquid Tanks and Its Effect on Ship Motions" , *Numerical simulations and experimental verification, RINA, Spring meeting*, (1984).
[19] Wagner, H. : Über Stoss- und Gleitvorgänge an der Oberflache von Flussigkeiten", *Zeitschr. F. Angew. Math. und Mech*., 12, pp. 193-235, (1932).
[20] Faltinsen, O.M., Rognebakke, O.F., Lukovsky, I.A., Timokha, A.N. : "Multidimensional Modal Analysis of Nonlinear Sloshing in a Rectangular Tank with Finite Water Depth" , *J. Fluid Mech*., Vol. 407, pp. 201-234, (2000).
[21] Faltinsen, O.M, and Timokha, A.N. : "Adaptive Multimodel Approach to Nonlinear Sloshing in a Rectangular Tank" , Submitted for publication, (2000).
[22] Rognebakke, O.F., and Faltinsen, O.M. : "Damping of Sloshing due to Tank Roof Impact" , *15th Int. Workshop on Water Waves and Floating Bodies, Caesarea, Israel*, (2000).
[23] Faltinsen, O.M., and Rognebakke, O.F. : "Sloshing and Slamming in Tanks" , *Hydronav'99-Manouevring'99, Gdansk-Ostrada, Poland*, (1999).
[24] Dobrovol'skaya, Z.N. : "On Some Problems of Similarity Flow of Fluid with a Free Surface" , *J. Fluid Mech*., Vol. 36, pp. 805-829, (1969).
[25] Faltinsen, O.M. : "Water Entry of a Wedge with Finite Deadrise Angle", to be published, (2000).
[26] Olsen, H., and Johnsen, K.R. : "Nonlinear Sloshing in Rectangular Tanks. A Pilot Study on the Applicability of Analytical Models", *Report No. 74-72-5*, Vol. 2, Det Norske Veritas, Høvik, Norway, (1975).